Experimental Characterization of Diversity Navigation

Andrea Conti, *Senior Member, IEEE*, Davide Dardari, *Senior Member, IEEE*, Matteo Guerra, Lorenzo Mucchi, *Senior Member, IEEE*, and Moe Z. Win, *Fellow, IEEE*

***Abstract*—Wireless networks with navigation capability enable mobile devices to both communicate and determine their positions. Diversity navigation employing multiple sensing technologies can overcome the limitation of individual technologies, especially when operating in harsh environments such as indoors. To characterize the diversity of navigation systems in real environments, we performed an extensive measurement campaign, where data from heterogenous sensors were collected simultaneously. The performance of Bayesian navigation algorithms, relying on the particle filter implementation, is evaluated based on measured data from ultrawideband, ZigBee, and inertial sensors. This enables us to quantify the benefits of data fusion as well as the effect of statistical mobility models for real-time diversity navigation.**

***Index Terms*—Diversity navigation, inertial devices, measurement campaign, mobility models, particle filters.**

I. Introduction

NETWORK NAVIGATION is a new trend on the horizon for future mobile technology, opening doors to a variety of navigation-based applications and services [1]. Examples include surveillance, medical therapy, traffic management, interactive remote control, and gaming [2].

The purpose of a navigation system is to determine the unknown position of mobile nodes (referred to as agents) based on measurements with respect to nodes in known positions (referred to as anchors) as well as other agents. Navigation performance is typically given in terms of localization error and outage (e.g., submeter localization error for at least 90% of positions in both space and time), as well as location-update rate (e.g., ten position estimates per second). These requirements, depending on specific applications, dictate the complexity of the navigation technique.

The most widely used solution to provide positional information is the global positioning system (GPS) which employs a constellation of satellites. In cluttered environments (e.g., inside buildings, in urban canyons, and under tree canopies), the GPS performance is often degraded due to propagation impairments such as multipath and line-of-sight (LOS) blockage. These impairments present significant challenges to the design and operation of indoor navigation systems.

The navigation process typically occurs in two phases: (i) a *measurement phase*, during which agents make intra- and/or internode measurements using different sensors, and (ii) a *location-update phase*, during which agents infer their positions based on prior knowledge and new measurements. Intranode measurements can be obtained through inertial measurement units (IMUs), which measure orientations, accelerations, and angular velocities, while internode measurements can be obtained through range measurement units (RMUs), which measure received signal strength (RSS) or time-of-arrival (TOA) of exchanged signals. Intranode measurements from IMUs can improve the performance of navigation systems by providing information on agents' mobility, especially when internode measurements exhibit a temporary outage due, for example, to obstacles. Examples of reliable internode measurements include ultrawideband (UWB) and narrowband signals from RMUs. Multipath resolvability of UWB signals [3]–[11] makes UWB-TOA-based technique ideal for high-accuracy ranging in cluttered environments [12]–[14]. ZigBee technology, designed for various wireless sensor network applications, can be used to infer distances through RSS measurements with low complexity [15]–[18]. The adoption of a single technology in harsh environments is often not sufficient to satisfy the accuracy and reliability requirement of the applications. To overcome these limitations, the use of multiple technologies for intra- and internode measurements is necessary, leading to *diversity navigation systems*. Bayesian filtering, based on mobility and perception models (also known as measurement models), can efficiently combine measurements from multiple sensors [19]. In particular, both mobility and perception models affect the navigation performance and need to be carefully characterized.

Recent research in localization and navigation has been carried out in three related strands, such as the following: (a) fundamental limits; (b) algorithm design; and (c) experimental

Manuscript received June 13, 2011; revised November 3, 2012 and December 28, 2012; accepted January 16, 2013. Date of publication August 15, 2013; date of current version February 5, 2014. This work was supported in part by the European Commission in the scope of the FP7 ICT project SELECT Grant 257544, by the Italian Ministero dello Sviluppo Economico under the project WEBS, by the Italian Ministero dell'Istruzione, dell'Università e della Ricerca under the project GRETA Grant 2010WHY5PR, by the Copernicus Fellowship, the Defense University Research Instrumentation Program under Grant N00014-08-1-0826, by the Korean National Research Foundation under Grant NRF-2011-220-D00076, by the National Science Foundation under Grant ECCS-0901034, by the Office of Naval Research under Grant N00014-11-1-0397, and by the MIT Institute for Soldier Nanotechnologies.

A. Conti and M. Guerra are with ENDIF, CNIT, University of Ferrara, 44122 Ferrara, Italy (e-mail: a.conti@ieee.org; matteo.guerra@unife.it).

D. Dardari is with DEI and WiLab, University of Bologna, 40136 Bologna, Italy (e-mail: ddardari@ieee.org).

L. Mucchi is with the DET, University of Firenze, 50139 Firenze, Italy (e-mail: lorenzo@ieee.org; http://lenst.det.unifi.it/~mucchi/index.html).

M. Z. Win is with the LIDS, Massachusetts Institute of Technology, Cambridge, MA 02139 USA (e-mail: moewin@mit.edu).

Color versions of one or more of the figures in this paper are available online at http://ieeexplore.ieee.org.

Digital Object Identifier 10.1109/JSYST.2013.2260638

characterization. Understanding the fundamentals of network localization and navigation is important not only to provide a performance benchmark but also to guide algorithm development and network design [20]–[29]. Given an underlaying technology, the localization and navigation performance also depends on the algorithm used [30]–[32]. The experimental characterization enables the system design for fulfilling the target performance in a real environment [33]–[36].

The design and analysis of diversity navigation systems in realistic environments require experiments specifically designed for collecting data from multiple sensing measurements under a common setting. While there are articles based on simulations using multiple RMUs [37] or measurements with single RMU and IMU as in [38], to the best of the authors' knowledge, there are no measurements from multiple RMUs and IMUs under a common setting, with a goal of characterizing diversity navigation systems.

In this paper, we characterize diversity navigation systems based on real-time measurements from multiple sensors in an indoor environment. In particular, we consider Bayesian (PFs) which combine the following: a prior knowledge from mobility and perception models; acceleration measurements from IMUs; and UWB impulse radio TOA and narrowband ZigBee RSS measurements from RMUs. The key contributions of this paper can be summarized as follows:

- introduction of mobility and perception models based on inertial and ranging measurements;
- comparison of mobility models under a common set of real-time indoor measurements;
- experimental characterization of diversity navigation systems employing multiple sensing technologies.

The remainder of this paper is organized as follows. The measurement campaign is described in Section II, Section III presents the Bayesian navigation algorithm, and Section IV reports the characterization of mobility and perception models based on experimental measurements. The performance metrics are defined in Section V, and the results of the navigation systems are given in Section VI. The conclusion is provided in Section VII.

II. Experimentation Setting

Here, we describe the measurement campaign that enables the comparison of various navigation techniques [39]. This campaign also allows us to quantify the benefits coming from different sensing technologies. In particular, we consider orientation and acceleration measurements using IMUs and UWB impulse radio TOA and narrowband ZigBee RSS measurements using RMUs. All measurements are taken automatically by a small robot moving at controlled speeds along a predetermined trajectory.

A. Measurement Setup

The experiment is performed in a typical office building located at the University of Bologna, Bologna, Italy. The map of the localization area, the trajectory of the robot, and the positions of the anchors are shown in Fig. 1. Note that the locations of the UWB anchors have been chosen to have most of the TOA-based ranging measurements taken in non-LOS conditions (worst case). Note also that the locations of ZigBee anchors and their number have been chosen to have a sufficient number of RSS-based ranging measurements taken in LOS conditions (otherwise, adequate ranging reliability would not be possible).

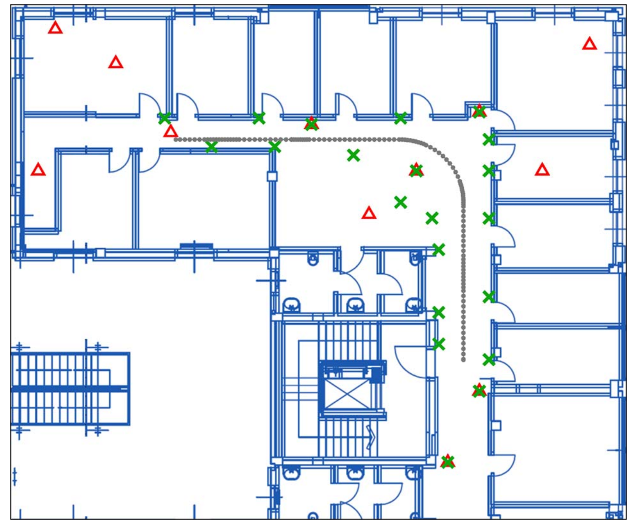

Fig. 1. Experimentation environment with UWB (triangles) and ZigBee (crosses) anchors. The trajectory of the robot is also depicted (gray curve).

The trajectory followed by the robot can be divided into three sections, with the total length equal to 18 m. The first section is a straight line along the y-axis, the second is a quarter of a circle with radius equal to 2.4 m, and the third is a straight line along the x-axis. Two different types of motion are considered: constant speed and variable speed. In both cases, the robot starts moving 5 s after the beginning of the experiment. In the constant-speed case, the robot travels the whole trajectory in 49.5 s with a speed of 0.36 m/s. In the variable-speed case, the robot is subjected to 14 different speeds. It travels the whole trajectory in 63.5 s with an average speed of 0.29 m/s and a maximum speed of 0.44 m/s.

B. Sensor Characteristics

The key sensing devices used in the measurement campaign consist of FCC-compliant UWB impulse radios, IEEE802.15.4-compliant narrowband ZigBee radios, and microelectromechanical systems (MEMS) based accelerometer. A brief description of these devices follows.

- FCC-compliant UWB devices: the UWB impulse radios operate with 3.2-GHz bandwidth centered at 4.6 GHz with -12.8 dBm of equivalent isotropically radiated power. Based on a proprietary protocol, two-way TOA-based range measurements between a pair of devices are collected every 500 ms.
- IEEE802.15.4-compliant ZigBee devices: these narrowband radios operate with 5-MHz bandwidth centered at 2.4 GHz. A total of 21 ZigBee devices are programmed as anchor nodes, while only one device is programmed as mobile node. Every 50 ms, the mobile node sends a broadcast message to the anchor nodes which perform the corresponding RSS measurements.

(a) (b)

Fig. 2. Views of the (a) robot carrying measurement devices and (b) experimentation environment.

- MEMS inertial sensing device: the accelerometer has a dynamic range up to $\pm 2g$ (g being the gravitational acceleration) with a 12-bit resolution. Every 2 ms, it acquires one acceleration measurement composed of three acceleration values, one for each axis.

A laptop is connected wirelessly to all of these devices for recording the measurements. Fig. 2(a) shows the robot carrying multiple sensing devices and moving along a programmed trajectory shown in Fig. 2(b). The motion and the speed of the robot are controlled through the laptop.

III. Bayesian Navigation

A navigation system can be modeled as a dynamic system, whose evolving state can include position, velocity, acceleration, and orientation. This state can be inferred from observations (i.e., the measurements) collected through multiple sensors using Bayesian filtering [19]. We now provide a survey on Bayesian navigation to recall the main aspects affecting the navigation performance.

A. Prediction and Correction Phases

The aim of navigation is to estimate the agent state $\mathbf{x}(t)$ at time t from multiple observations and prior knowledge. The observations are collected in discrete times $\{t_k\}$ with interval $\Delta_\mathrm{t} = t_k - t_{k-1}$ for all $k = 1, 2, \ldots, K$; hence, the agent state is updated every Δ_t seconds. We use the notation $\mathbf{x}_k = \mathbf{x}(t)k$ and denote $\mathbf{z}_k = [z_{k,1}, z_{k,2}, \ldots, z_{k,N_k}]$ as the set of N_k observations at time t_k.[1] The Bayesian filters estimate a probability density function (pdf) $b(\mathbf{x}_k)$ of $\mathbf{x}_k$, called belief, over the state space conditioned on all collected observations. To illustrate, we denote $\mathbf{z}_{1:k}$ as the sequence of all observations until the time t_k. The belief $b(\mathbf{x}_k)$ is then defined as the pdf of the random variable $\mathbf{x}_k$ conditioned on all the observations up to time t_k as given by

$$b(\mathbf{x}_k) = f(\mathbf{x}_k|\mathbf{z}_{1:k})\,. \tag{1}$$

[1]For instance, the agent state $\mathbf{x}_k$ at time k consists of position $\mathbf{p}_k$ and velocity $\mathbf{v}_k$, whose estimates will be denoted by $\hat{\mathbf{p}}_k$ and $\hat{\mathbf{v}}_k$, respectively.

The state $\mathbf{x}_k$ based on observations $\mathbf{z}_{1:k}$ can be estimated from (1) via maximum a posteriori estimation. To make the computation tractable, we consider that the dynamic system is modeled as a first-order Markov chain [19]. This implies that the inference of the state $\mathbf{x}_k$ is based on the previous state $\mathbf{x}_{k-1}$ and can be described as a succession of prediction and correction phases.

We now discuss the prediction and the correction phases for inferring the new state. Given the belief $b(\mathbf{x}_{k-1}) = f(\mathbf{x}_{k-1}|\mathbf{z}_{1:k-1})$ at time t_{k-1}, the *predicted* belief at time t_k is given by

$$b^-(\mathbf{x}_k) = f(\mathbf{x}_k|\mathbf{z}_{1:k-1}) = \int f_\mathrm{m}(\mathbf{x}_k|\mathbf{x}_{k-1}) b(\mathbf{x}_{k-1}) d\mathbf{x}_{k-1} \tag{2}$$

where the term $f_\mathrm{m}(\mathbf{x}_k|\mathbf{x}_{k-1})$ is the *mobility model* of the agent. The mobility model gives the pdf of current position $\mathbf{x}_k$ given the previous position $\mathbf{x}_{k-1}$, and it is related to the environment and the mobility behavior of the agent.

When a new set of measurements is collected, the *updated* belief is given via Bayes' rule

$$b(\mathbf{x}_k) = \eta f_\mathrm{p}(\mathbf{z}_k|\mathbf{x}_k) b^-(\mathbf{x}_k) \tag{3}$$

where $\eta = 1/f(\mathbf{z}_k|\mathbf{z}_{1:k-1})$ and the term $f_\mathrm{p}(\mathbf{z}_k|\mathbf{x}_k)$ is the *perception model* of the agent. The perception model gives the pdf of observations $\mathbf{z}_k$ given the position $\mathbf{x}_k$ and is related to the environment and sensor technology.

B. Bayesian Particle Filters

Bayesian filters differ in the representation of the pdf for each state $\mathbf{x}_k$. Among several implementations, those based on PFs provide a good compromise in terms of complexity, flexibility, and accuracy [2].

Belief computation via PFs is based on a sampling procedure known as (SIS) [40]. The key advantage is the ability to represent an arbitrary pdf by using more particles into regions of the state space having higher probability. The PF implementation requires attention when applied to high-dimensional estimation problems since the complexity grows exponentially with the dimension of the state space.

PFs are based on sets of samples weighted according to the belief $b(\mathbf{x}_k)$ which is thus approximated as

$$b(\mathbf{x}_k) \approx \sum_{i=1}^{N_\mathrm{s}} w_{k,i}\delta(\mathbf{x}_k - \mathbf{x}_{k,i}) \tag{4}$$

where N_s is the number of particles, $w_{k,i} \geq 0\, \forall i, k$ is the weight for particle i at time t_k such that $\sum_{i=1}^{N_\mathrm{s}} w_{k,i} = 1$, and $\delta(\cdot)$ is the Dirac's delta pseudofunction. The quality of the approximation in (4) depends on the number of particles N_s. According to [40], a way to compute (4) is given by

$$\mathbf{x}_{k,i} \sim f_\mathrm{m}(\mathbf{x}_{k,i}|\mathbf{x}_{k-1,i}) \quad \text{mobility model} \tag{5}$$
$$w_{k,i} = w_{k-1,i} f_\mathrm{p}(\mathbf{z}_k|\mathbf{x}_{k,i}) \quad \text{perception model.} \tag{6}$$

After several iterations, only a few particles might have nonnegligible weight. To overcome this problem, a resampling enables us to delete the inconsistent samples (those with negligible weights) and to increase the number of particles with high weights. This procedure is known as sequential importance resempling (SIR) [40].

IV. Mobility and Perception Models

We now present the mobility and perception models whose parameters are characterized based on inertial and ranging measurements. Our approach evaluates the belief of state $\mathbf{x}_k$, which is given by position $\mathbf{p}_k$, and takes the velocity $\mathbf{v}_k$ into account through the mobility model.

A. Mobility Models

The mobility model for each agent depends on its movement capability in the environment and the specific application. We consider Gaussian mobility models with conditional pdf of $\mathbf{p}_{k,i}$, conditioned on the previous position $\mathbf{p}_{k-1,i}$, given by[2]

$$f_\mathrm{m}(\mathbf{p}_{k,i}|\mathbf{p}_{k-1,i}) = \frac{1}{2\pi|\boldsymbol{\Sigma}_\mathrm{m}|^{\frac{1}{2}}} e^{-\frac{1}{2}\left[(\mathbf{p}_{k,i}-\boldsymbol{\mu}_{k,i})^\mathrm{T}\boldsymbol{\Sigma}_\mathrm{m}^{-1}(\mathbf{p}_{k,i}-\boldsymbol{\mu}_{k,i})\right]} \tag{7}$$

where $\boldsymbol{\mu}_{k,i}$ varies with the mobility model, as described in the following, and the covariance matrix $\boldsymbol{\Sigma}_\mathrm{m}$ accounts for the uncertainty in the movements in a 2-D plane; thus, it is expressed by

$$\boldsymbol{\Sigma}_\mathrm{m} = \begin{bmatrix} \sigma_{\mathrm{m},x}^2 & \rho\,\sigma_{\mathrm{m},x}\sigma_{\mathrm{m},y} \\ \rho\,\sigma_{\mathrm{m},x}\sigma_{\mathrm{m},y} & \sigma_{\mathrm{m},y}^2 \end{bmatrix}. \tag{8}$$

We propose two mobility models based on (7), namely, mobility with speed measurements and mobility with speed learning. They are described in the following together with the case of absence of mobility.

1) *Mobility with speed measurement* (SM). When the speed and the direction of the motion are measured from an IMU, the mean $\boldsymbol{\mu}_{k,i}$ in (7) depends on $\mathbf{p}_{k-1,i}$, and the speed $\mathbf{v}_{k-1}$ is measured at time t_{k-1} according to

$$\boldsymbol{\mu}_{k,i} = \mathbf{p}_{k-1,i} + \mathbf{v}_{k-1}\Delta_\mathrm{t}. \tag{9}$$

The standard deviations $\sigma_{\mathrm{m},x}$ and $\sigma_{\mathrm{m},y}$ on the two axes are computed starting from the measurement accuracy of the IMU device.

2) *Mobility with speed learning* (SL). When the speed and the direction of the motion are determined from previously estimated positions, a sliding window of N_ν previous estimated positions can be used, and the mean $\boldsymbol{\mu}_{k,i}$ in (7) is obtained as in (9) with

$$\mathbf{v}_{k-1} = \frac{1}{N_\nu\Delta_\mathrm{t}}\sum_{j=1}^{N_\nu}(\hat{\mathbf{p}}_{k-j} - \hat{\mathbf{p}}_{k-j-1}) = \frac{1}{N_\nu\Delta_\mathrm{t}}(\hat{\mathbf{p}}_{k-1} - \hat{\mathbf{p}}_{k-N_\nu-1}). \tag{10}$$

We will compare the SM and SL mobility models under the same $\sigma_{\mathrm{m},x}$ and $\sigma_{\mathrm{m},y}$.

3) *No mobility* (NM). When the position at each instant is estimated independently of the previous one, navigation reduces to a sequence of independent localization steps. Therefore, the mobility model is given by

$$f_\mathrm{m}(\mathbf{p}_{k,i}|\mathbf{p}_{k-1,i}) = \frac{1}{|\mathcal{S}|}\mathbb{1}_\mathcal{S}(\mathbf{p}_{k,i}) \tag{11}$$

where $\mathcal{S} \in \mathbb{R}^2$ is the set of possible 2-D locations within the experimentation area with size $|\mathcal{S}|$ and $\mathbb{1}_\mathcal{S}(\mathbf{p}) = 1$ for $\mathbf{p} \in \mathcal{S}$ and 0 otherwise.

B. Perception Models

We denote the coordinates of UWB anchor nodes by $\mathbf{p}_n^{(\mathrm{U})}$, for $n = 1, 2, \ldots, N_\mathrm{b}^{(\mathrm{U})}$, and the coordinates of ZigBee anchor nodes by $\mathbf{p}_m^{(\mathrm{Z})}$, for $m = 1, 2, \ldots, N_\mathrm{b}^{(\mathrm{Z})}$. The observation vector $\mathbf{z}_k$ is defined as

$$\mathbf{z}_k = \begin{bmatrix}\mathbf{r}_k^{(\mathrm{U})} \\ \mathbf{r}_k^{(\mathrm{Z})}\end{bmatrix} \tag{12}$$

where $\mathbf{r}_k^{(\mathrm{U})}$ and $\mathbf{r}_k^{(\mathrm{Z})}$ represent the range measurement vectors from UWB and ZigBee anchor nodes at time t_k, respectively. We consider a perception model (6), with independent observations, given by

$$f_\mathrm{p}(\mathbf{z}_k|\mathbf{p}_{k,i}) = \prod_{n\in\mathcal{C}_k^{(\mathrm{U})}} f_\mathrm{U}\left(r_{k,n}^{(\mathrm{U})}|\mathbf{p}_{k,i}\right) \times \prod_{m\in\mathcal{C}_k^{(\mathrm{Z})}} f_\mathrm{Z}\left(r_{k,m}^{(\mathrm{Z})}|\mathbf{p}_{k,i}\right) \tag{13}$$

where $r_{k,n}^{(\mathrm{U})}$, element of $\mathbf{r}_k^{(\mathrm{U})}$, and $r_{k,m}^{(\mathrm{Z})}$, element of $\mathbf{r}_k^{(\mathrm{Z})}$, are range measurements at time t_k from the UWB anchor n and the ZigBee anchor m, respectively. The sets $\mathcal{C}_k^{(\mathrm{U})}$ and $\mathcal{C}_k^{(\mathrm{Z})}$ contain the indexes of UWB and ZigBee neighboring anchor nodes at time t_k, respectively. The likelihood functions f_U and f_Z are assumed to be Gaussian distributions, resulting in

$$f_\mathrm{U}\left(r_{k,n}^{(\mathrm{U})}|\mathbf{p}_{k,i}\right) \sim \mathcal{N}\left(\left\|\mathbf{p}_{k,i} - \mathbf{p}_n^{(\mathrm{U})}\right\|, \sigma_\mathrm{p}^{(\mathrm{U})2}\right) \tag{14}$$

$$f_\mathrm{Z}\left(r_{k,m}^{(\mathrm{Z})}|\mathbf{p}_{k,i}\right) \sim \mathcal{N}\left(\left\|\mathbf{p}_{k,i} - \mathbf{p}_m^{(\mathrm{Z})}\right\|, \sigma_\mathrm{p}^{(\mathrm{Z})2}\right). \tag{15}$$

[2]In the absence of prior information on the real movement of the agent (i.e., the agent is free to move in all directions with different speeds), the Gaussian mobility model represents a fairly general model with a tractable number of parameters. In the presence of some prior information on the agent's movement (e.g., direction or speed is set by the environment), a mobility model more tight to the real mobility would provide better performance.

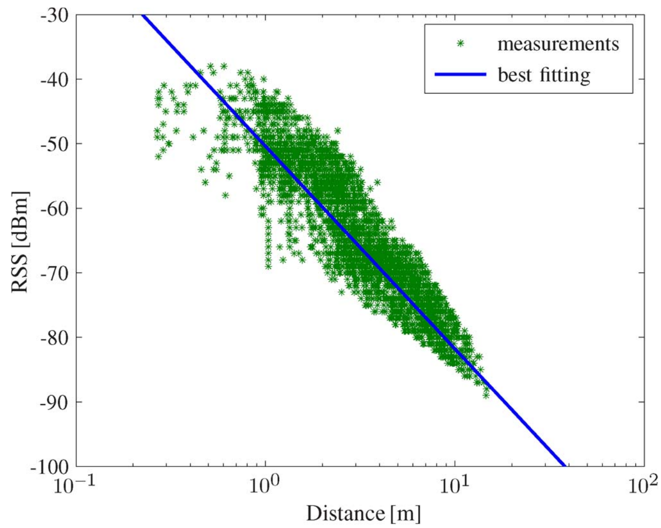

Fig. 3. Measured RSS as a function of the true distance. Best fitting curve is reported with $P_0 = -50.4$ dBm and $\beta = 3.14$.

The standard deviations $\sigma_{\rm p}^{(\rm U)}$ and $\sigma_{\rm p}^{(\rm Z)}$ depend on the sensing technology and can be obtained from measurements (e.g., see the network experimentation methodology introduced in [36]).

Ranging techniques significantly affect the localization accuracy, system complexity, and system cost. We now discuss briefly how to estimate the range from measurements obtained with the RMUs in the experimental campaign.

In the experimental campaign, UWB nodes measure the round-trip time $\tau_{\rm RT}$, which is related to the TOF $\tau_{\rm f}$ by

$$\tau_{\rm RT} = 2\tau_{\rm f} + \tau_{\rm d} \tag{16}$$

where $\tau_{\rm d}$ is the response delay of the involved node.[3] The distance r between two nodes can be determined by $(\tau_{\rm RT} - \tau_{\rm d})c/2$, where c is the speed of electromagnetic waves.

From RSS measurements between two nodes, the distance can be estimated for a known propagation model. The presence of propagation effects such as small-scale and large-scale fadings makes the received power stochastic. The mapping of the RSS from a ZigBee device into a distance requires a deterministic model, which is typically obtained by fitting the measurements in the experimentation with appropriate regression model [16]. We consider a deterministic regression model for which the received power $P_{\rm r}$ (the RSS in dBm) is related to the distance r (in meters) as

$$P_{\rm r} = P_0 - 10\beta \log\left(\frac{r}{r_0}\right) \tag{17}$$

where P_0 (dBm) is the power received at a distance r_0 and β is the path loss exponent. Parameters P_0 and β have been obtained through best fitting with measurements, as shown in Fig. 3. Therefore, from measured $P_{\rm r}$, the expression

$$r = r_0 10^{-\frac{P_{\rm r}-P_0}{10\beta}} \tag{18}$$

can be used to determine the distance between the two nodes.

[3]A two-way ranging protocol is employed; therefore, synchronization between the two nodes is not required [13].

V. Performance Metrics

We now define the performance metrics for characterizing diversity navigation systems. The navigation error, at time t_k, is given by

$$e(\mathbf{p}_k) = \|\hat{\mathbf{p}}_k - \mathbf{p}_k\| \tag{19}$$

which represents the Euclidean distance between the estimated position $\hat{\mathbf{p}}_k$ and the true position $\mathbf{p}_k$ at time t_k.

Based on (19), the navigation root mean square error (RMSE) $e_{\rm RMS}$ is defined as

$$e_{\rm RMS} = \sqrt{\mathbb{E}\left\{e(\mathbf{p}_k)^2\right\}} \tag{20}$$

where $\mathbb{E}\{\cdot\}$ represents the statistical expectation over the ensemble of space and time. The performance can be also characterized in terms of navigation error outage (NEO) which is defined as the navigation-error-based outage probability (OP), which is given by[4]

$$\begin{aligned} P_{\rm NEO} &= \mathbb{P}\left\{e(\mathbf{p}_k) > e_{\rm th}\right\} \\ &= \mathbb{E}\left\{\mathbb{1}_{(e_{\rm th},+\infty)}\left(\|\hat{\mathbf{p}}_k - \mathbf{p}_k\|\right)\right\}. \end{aligned} \tag{21}$$

In (21), $e_{\rm th}$ is the application-dependent target (i.e., the maximum tolerable) localization error, and $\mathbb{1}_{\mathcal{A}}(x) = 1$ when $x \in \mathcal{A}$ and 0 otherwise. The NEO can be interpreted as the probability that the localization error at a particular position exceeds the target localization error $e_{\rm th}$ as the agent moves along the trajectory.

VI. Experimental Results

This section provides results for a diversity navigation system based on measurements. Navigation accuracy is evaluated in terms of navigation RMSE $e_{\rm RMS}$ and NEO $P_{\rm NEO}$,[5] as discussed in Section V, for Bayesian PFs employing the mobility and perception models described in Section IV. In particular, mobility models NM, SM, and SL are considered for both cases of constant and variable speeds. The number of particles $N_{\rm s}$ influences the accuracy of the position estimate as well as the complexity of the algorithm. To determine a good tradeoff between performance and complexity, we evaluate the navigation performance with different values of $N_{\rm s}$. In Fig. 4, we show the NEO for different numbers of particles, employing the mobility model SL with only UWB devices in variable-speed scenario. This result allows us to understand the benefit of increasing the number of particles. In our evaluation, the performance improvement saturates at a value of about $N_{\rm s} = 1000$. The parameter settings used for the navigation algorithm are reported in Table I, where we assume for the covariance matrix in (8) that the coordinates are independent (i.e., $\rho = 0$) with the same standard deviation $\sigma_{{\rm m},x} = \sigma_{{\rm m},y} = \sigma_{\rm m}$.

[4]The OP is a well-known concept in wireless communications; the similarity with the application to location-aware networks is in evaluating the probability that the quality of service falls below a given target value [41].

[5]In the numerical results, $P_{\rm NEO}$ has to be interpreted as an outage rate in the given mobility path shown in Fig. 1.

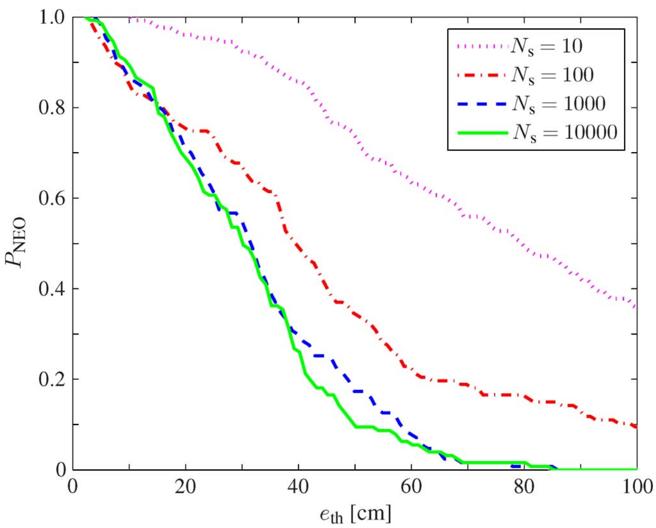

Fig. 4. NEO versus e_{th} (in centimeters) with $\Delta_t = 500$ ms for different values of N_s. The SL model is considered with $\sigma_m = 0.04$ m and $N_\nu = 20$.

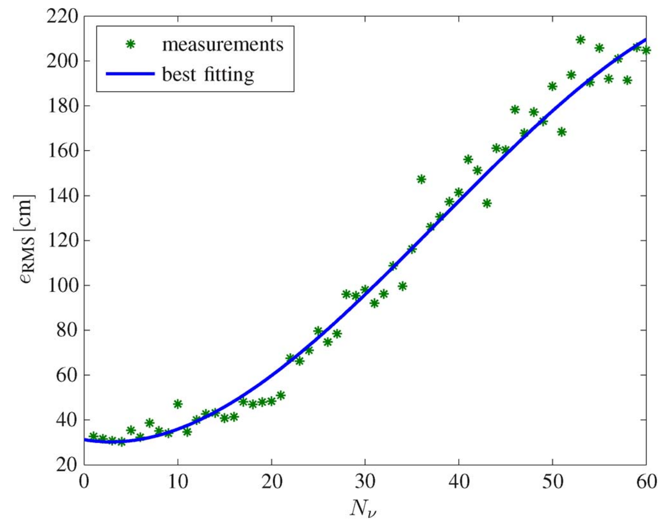

Fig. 5. Navigation RMSE as a function of window size N_ν for the UWB system and mobility model SL. A constant-speed scenario is considered.

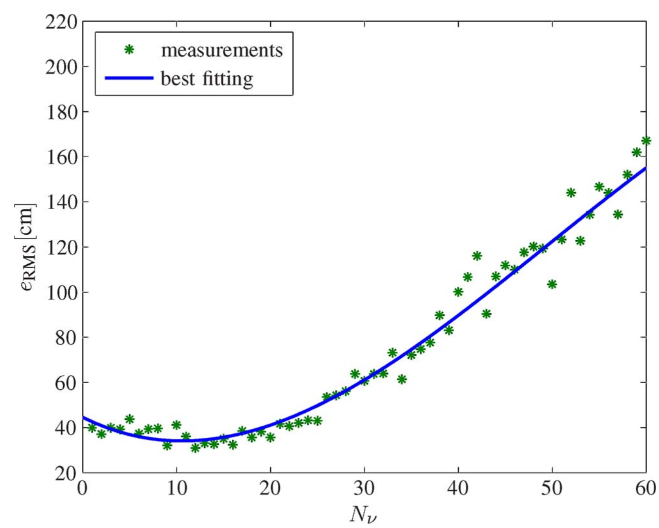

Fig. 6. Navigation RMSE as a function of window size N_ν for the UWB system and mobility model SL. A variable-speed scenario is considered.

TABLE I
PARAMETER SETTINGS FOR THE NAVIGATION ALGORITHM

Parameter	Value	Technique
N_s	1000	ALL
Δ_t	500 ms	ALL
σ_m	0.04 m	SM-SL
β	3.14	ZigBee
P_0	−50.4 dBm	ZigBee
$\sigma_p^{(U)}$	0.26 m	UWB
$\sigma_p^{(Z)}$	0.50 m	ZigBee

TABLE II
NEO AND e_{RMS} FOR THE BAYESIAN PFS WHEN ONLY THE UWB NAVIGATION. MOBILITY MODELS NM, SM, AND SL WITH OPTIMUM WINDOW SIZE ARE CONSIDERED WITH CONSTANT SPEED

Mobility Model	$P_{\mathbf{NEO}}(1\text{ m})$	$P_{\mathbf{NEO}}(0.5\text{ m})$	$e_{\mathbf{RMS}}$ [cm]
NM	0.03	0.28	54.64
SM	0	0.22	40.00
SL	0	0.20	39.53

TABLE III
NEO AND e_{RMS} FOR THE BAYESIAN PFS WHEN ONLY THE UWB NAVIGATION. MOBILITY MODELS NM, SM, AND SL WITH OPTIMUM WINDOW SIZE ARE CONSIDERED WITH VARIABLE SPEED

Mobility Model	$P_{\mathbf{NEO}}(1\text{ m})$	$P_{\mathbf{NEO}}(0.5\text{ m})$	$e_{\mathbf{RMS}}$ [cm]
NM	0.12	0.32	109.43
SM	0	0.07	29.93
SL	0.01	0.15	37.81

The effect of the window size N_ν on the navigation RMSE e_{RMS} for the mobility model SL is evaluated in Figs. 5 and 6 for the constant- and variable-speed cases, respectively. Experimental data are reported together with the fitting curve. These figures show a tradeoff between the capabilities of the SL model to filter measurement noise and to follow agent accelerations. In fact, for lower N_ν, the mobility model suffers from measurements noise, while for higher values, the speed is averaged over a window length that does not enable to follow rapid accelerations. In the case of variable speed, the optimum window size for SL is approximately $N_\nu = 10$, whereas the navigation RMSE remains almost constant for lower values until $N_\nu = 7$ and 8 in the case of constant speed.

The NEO and navigation RMSE for UWB technology are reported in Tables II and III for the cases of constant speed and variable speed, respectively. From Tables II and III, one can see the improved navigation performance when the mobility models SM and SL are used, especially for the case of variable speed. The RMSE in the two tables shows how a statistical mobility model with estimation or measurement of the speed vector of the agent improves the navigation performance.

The NEOs of Bayesian PFs employing the mobility models NM, SM, and SL (with optimum window size) are shown in Figs. 7 and 8 for the cases of constant speed and variable speed, respectively. Note that the NEO is significantly affected by the mobility model, especially in the case of variable speed. For example, Fig. 8 indicates that, in 80% of cases, the navigation errors are below 35 and 43 cm for SM and SL, respectively, while with NM, it is below 73 cm for the case of variable speed.

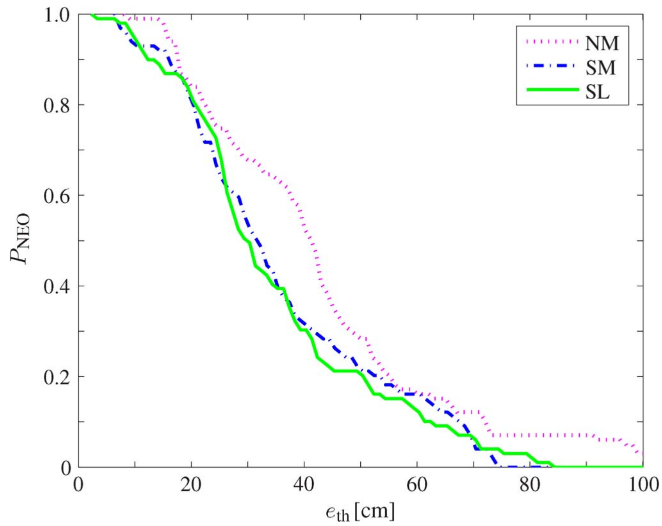

Fig. 7. NEO for the UWB system. Constant-speed scenario. Three mobility models: NM, SM, and SL with optimum window size.

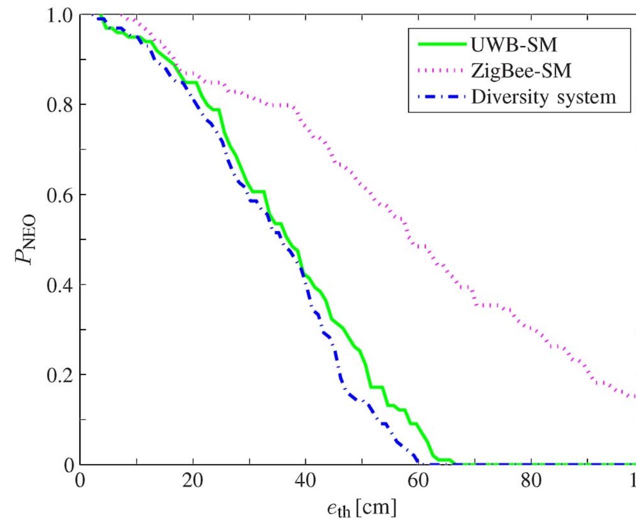

Fig. 9. NEO for UWB, ZigBee, and diversity systems. A constant-speed scenario is considered.

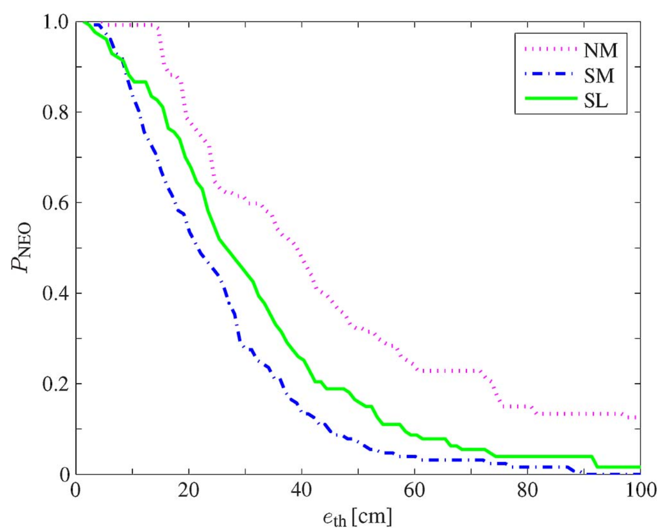

Fig. 8. NEO for the UWB system. Variable-speed scenario. Three mobility models: NM, SM, and SL with optimum window size.

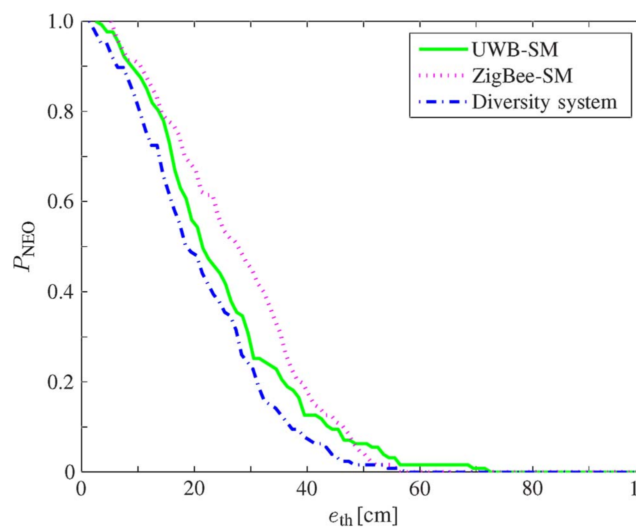

Fig. 10. NEO for UWB, ZigBee, and diversity systems. A variable-speed scenario is considered.

We now present results for the ZigBee ranging unit only and for a diversity navigation system fusing UWB, ZigBee, and inertial measurements. In particular, Figs. 9 and 10 show the NEO for mobility model SM in the cases of constant and variable speeds, respectively. Note that the diversity solution with joint use of UWB, ZigBee, and inertial sensors improves the performance, especially in the case of variable speed. The diversity system captures the benefits of both single technologies, especially in the case of constant speed where the ZigBee measurements are inaccurate. Tables IV and V report the NEO and navigation RMSE; as example in the case of variable speed, the joint usage of the three sensing technologies ameliorates the navigation RMSE of about 20% with respect to the UWB or ZigBee system alone. Figure 11 and Table VI illustrate the diversity system and the mobility models NM and SL when both UWB and ZigBee technologies are employed. Results show how diversity schemes lead to a larger performance improvement in terms of both e_{RMS} and NEO. An example of estimated trajectory with the diversity navigation system is given in Fig. 12 for the case of variable speed.

TABLE IV
NEO AND e_{RMS} FOR THE BAYESIAN PFS WHEN UWB, ZIGBEE, AND DIVERSITY SYSTEMS ARE EMPLOYED. MODEL SM IS CONSIDERED WITH CONSTANT SPEED

Technology	$P_{\textbf{NEO}}(1\,\text{m})$	$P_{\textbf{NEO}}(0.5\,\text{m})$	$e_{\textbf{RMS}}$ [cm]
UWB-SM	0	0.27	42.12
ZigBee-SM	0.15	0.68	69.00
Diversity system	0	0.22	40.02

VII. CONCLUSION

Diversity navigation systems enable new applications that require high-accuracy localization of mobile nodes even in harsh environments. We have characterized a diversity navigation system based on measurements from multiple sensor

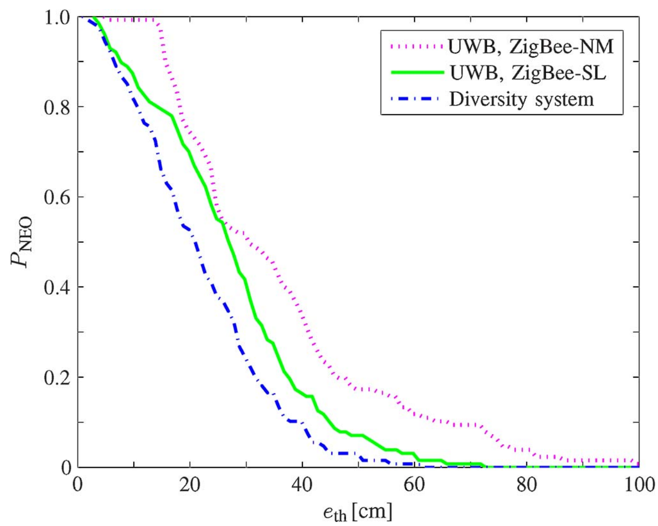

Fig. 11. NEO for UWB and ZigBee technologies with models NM, SL, and SM in variable-speed scenario. Optimum window size is considered for SL.

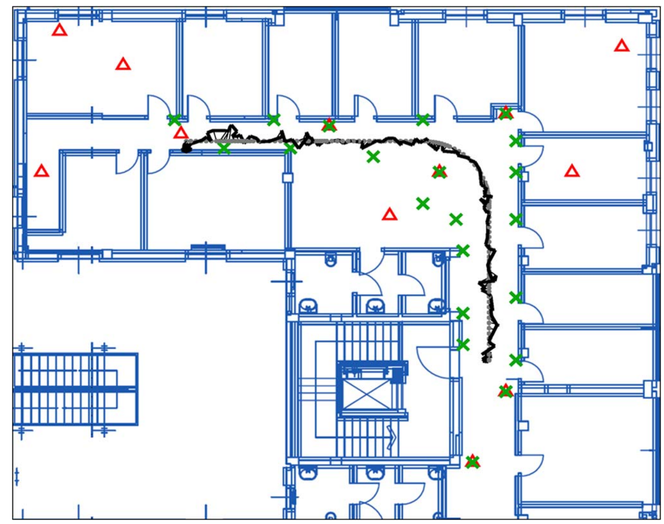

Fig. 12. Real (gray) and estimated (black) trajectories of the robot for the diversity navigation system. UWB (triangles) and ZigBee (crosses) anchors are indicated.

TABLE V

NEO AND e_{RMS} FOR THE BAYESIAN PFs WHEN UWB, ZIGBEE, AND DIVERSITY SYSTEMS ARE EMPLOYED. MODEL SM IS CONSIDERED WITH VARIABLE SPEED

Technology	$P_{\mathbf{NEO}}(1\,\mathrm{m})$	$P_{\mathbf{NEO}}(0.5\,\mathrm{m})$	$e_{\mathbf{RMS}}$ [cm]
UWB-SM	0	0.07	29.01
ZigBee-SM	0	0.06	30.00
Diversity system	0	0.02	24.12

TABLE VI

NEO AND e_{RMS} FOR THE BAYESIAN PFs WHEN UWB AND ZIGBEE TECHNOLOGIES ARE EMPLOYED. MODELS NM, SL, AND SM ARE CONSIDERED WITH VARIABLE SPEED

Technology	$P_{\mathbf{NEO}}(1\,\mathrm{m})$	$P_{\mathbf{NEO}}(0.5\,\mathrm{m})$	$e_{\mathbf{RMS}}$ [cm]
UWB, ZigBee-NM	0.01	0.17	41.16
UWB, ZigBee-SL	0	0.07	30.62
Diversity system	0	0.02	24.12

technologies under a common setting. The navigation performance of Bayesian particle filtering of measurements from UWB, ZigBee, and inertial sensors has been determined in terms of navigation error and NEO. Various mobility and perception models have been used in Bayesian filtering with parameters determined from measurements. Our results have shown that the diversity solution can improve the navigation accuracy, especially with variable speed. Experimental results provide insights on how and when mobility information can be harnessed to ameliorate the navigation performance.

ACKNOWLEDGMENT

The authors would like to thank M. Chiani for hosting the experimentation and N. Decarli and colleagues of NEWCOM++ WPR.B for their participation in the measurement campaign. The measurement campaign has been realized in the framework of the European Network of Excellence NEWCOM++.

REFERENCES

[1] M. Z. Win, A. Conti, S. Mazuelas, Y. Shen, W. M. Gifford, D. Dardari, and M. Chiani, "Network localization and navigation via cooperation," *IEEE Commun. Mag.*, vol. 49, no. 5, pp. 56–62, May 2011.

[2] D. Dardari, E. Falletti, and M. Luise, *Satellite and Terrestrial Radio Positioning Techniques—A signal processing perspective*. London, U.K.: Elsevier, 2011.

[3] M. Z. Win and R. A. Scholtz, "Impulse radio: How it works," *IEEE Commun. Lett.*, vol. 2, no. 2, pp. 36–38, Feb. 1998.

[4] M. Z. Win and R. A. Scholtz, "Ultra-wide bandwidth time-hopping spread-spectrum impulse radio for wireless multiple-access communications," *IEEE Trans. Commun.*, vol. 48, no. 4, pp. 679–689, Apr. 2000.

[5] A. F. Molisch, "Ultra-wide-band propagation channels," *Proc. IEEE*, vol. 97, no. 2, pp. 353–371, Feb. 2009.

[6] L. Yang and G. B. Giannakis, "Optimal pilot waveform assisted modulation for ultrawideband communications," *IEEE Trans. Wireless Commun.*, vol. 3, no. 4, pp. 1236–1249, Jul. 2004.

[7] M. Z. Win and R. A. Scholtz, "On the robustness of ultra-wide bandwidth signals in dense multipath environments," *IEEE Commun. Lett.*, vol. 2, no. 2, pp. 51–53, Feb. 1998.

[8] M. Z. Win and R. A. Scholtz, "Characterization of ultra-wide bandwidth wireless indoor communications channel: A communication theoretic view," *IEEE J. Sel. Areas Commun.*, vol. 20, no. 9, pp. 1613–1627, Dec. 2002.

[9] A. F. Molisch, "Ultrawideband propagation channels-theory, measurement, and modeling," *IEEE Trans. Veh. Technol.*, vol. 54, no. 5, pp. 1528–1545, Sep. 2005.

[10] A. F. Molisch, D. Cassioli, C.-C. Chong, S. Emami, A. Fort, B. Kannan, J. Karedal, J. Kunisch, H. Schantz, K. Siwiak, and M. Z. Win, "A comprehensive standardized model for ultrawideband propagation channels," *IEEE Trans. Antennas Propag.*, vol. 54, no. 11, pp. 3151–3166, Nov. 2006.

[11] S. Gezici, Z. Tian, G. B. Giannakis, H. Kobayashi, A. F. Molisch, H. V. Poor, and Z. Sahinoglu, "Localization via ultra-wideband radios: A look at positioning aspects for future sensor networks," *IEEE Signal Process. Mag.*, vol. 22, no. 4, pp. 70–84, Jul. 2005.

[12] J.-Y. Lee and R. A. Scholtz, "Ranging in a dense multipath environment using an UWB radio link," *IEEE J. Sel. Areas Commun.*, vol. 20, no. 9, pp. 1677–1683, Dec. 2002.

[13] D. Dardari, A. Conti, U. J. Ferner, A. Giorgetti, and M. Z. Win, "Ranging with ultrawide bandwidth signals in multipath environments," *Proc. IEEE*, vol. 97, no. 2, pp. 404–426, Feb. 2009.

[14] K. Yu and I. Oppermann, "Performance of UWB position estimation based on time-of-arrival measurements," in *Proc. Int. Workshop Ultra Wideband Syst.*, Oulu, Finland, May 2004, pp. 400–404.

[15] R. Verdone, D. Dardari, G. Mazzini, and A. Conti, *Wireless Sensor and Actuator Networks: Technologies, Analysis and Design*. London, U.K.: Elsevier, 2008.

[16] T. Pavani, G. Costa, M. Mazzotti, A. Conti, and D. Dardari, "Experimental results on indoor localization techniques through wireless sensors network," in *Proc. IEEE Semiannu. Veh. Technol. Conf.*, Melbourne, Australia, May 2006, vol. 2, pp. 663–667.

[17] S. Mazuelas, A. Bahillo, R. Lorenzo, P. Fernandez, F. A. Lago, E. Garcia, J. Blas, and E. Abril, "Robust indoor positioning provided by real-time RSSI values in unmodified WLAN networks," *IEEE J. Sel. Topics Signal Process.*, vol. 3, no. 5, pp. 821–831, Oct. 2009.
[18] S. Severi, G. Liva, M. Chiani, and D. Dardari, "A new low-complexity user tracking algorithm for WLAN-based positioning systems," in *Proc. Mobile Wireless Commun. Summit*, Jul. 2007, pp. 1–5.
[19] D. Fox, J. Hightower, L. Liao, D. Schulz, and G. Borriello, "Bayesian filtering for location estimation," *IEEE Pervasive Comput.*, vol. 2, no. 3, pp. 24–33, Jul./Sep. 2003.
[20] M. J. D. Rendas and J. M. F. Moura, "Cramér–Rao bound for location systems in multipath environments," *IEEE Trans. Signal Process.*, vol. 39, no. 12, pp. 2593–2610, Dec. 1991.
[21] Y. Shen and M. Z. Win, "On the accuracy of localization systems using wideband antenna arrays," *IEEE Trans. Commun.*, vol. 58, no. 1, pp. 270–280, Jan. 2010.
[22] E. G. Larsson, "Cramér–Rao bound analysis of distributed positioning in sensor networks," *IEEE Signal Process. Lett.*, vol. 11, no. 3, pp. 334–337, Mar. 2004.
[23] D. B. Jourdan, D. Dardari, and M. Z. Win, "Position error bound for UWB localization in dense cluttered environments," *IEEE Trans. Aerosp. Electron. Syst.*, vol. 44, no. 2, pp. 613–628, Apr. 2008.
[24] L. Mailaender, "On the geolocation bounds for round-trip time-of-arrival and all non-line-of-sight channels," *EURASIP J. Adv. Signal Process.*, vol. 2008, no. 1, pp. 584 670-1–584 670-10, Nov. 2008.
[25] Y. Shen and M. Z. Win, "Fundamental limits of wideband localization—Part I: A general framework," *IEEE Trans. Inf. Theory*, vol. 56, no. 10, pp. 4956–4980, Oct. 2010.
[26] Y. Shen, H. Wymeersch, and M. Z. Win, "Fundamental limits of wideband localization—Part II: Cooperative networks," *IEEE Trans. Inf. Theory*, vol. 56, no. 10, pp. 4981–5000, Oct. 2010.
[27] H. Godrich, A. Petropulu, and H. V. Poor, "Power allocation strategies for target localization in distributed multiple-radar architectures," *IEEE Trans. Signal Process.*, vol. 59, no. 7, pp. 3226–3240, Jul. 2011.
[28] Y. Shen, S. Mazuelas, and M. Z. Win, "Network navigation: Theory and interpretation," *IEEE J. Sel. Areas Commun.*, vol. 30, no. 9, pp. 1823–1834, Oct. 2012.
[29] Y. Karisan, D. Dardari, S. Gezici, A. A. D'Amico, and U. Mengali, "Range estimation in multicarrier systems in the presence of interference: Performance limits and optimal signal design," *IEEE Trans. Wireless Commun.*, vol. 10, no. 10, pp. 3321–3331, Oct. 2011.
[30] H. Wymeersch, J. Lien, and M. Z. Win, "Cooperative localization in wireless networks," *Proc. IEEE*, vol. 97, no. 2, pp. 427–450, Feb. 2009.
[31] U. A. Khan, S. Khar, and J. M. F. Moura, "DILAND: An algorithm for distributed sensor localization with noisy distance measurements," *IEEE Trans. Signal Process.*, vol. 58, no. 3, pp. 1940–1947, Mar. 2010.
[32] T. Sathyan and M. Hedley, "Efficient particle filtering for tracking maneuvering object," in *Proc. IEEE/ION PLANS*, May 2010, pp. 332–339.
[33] D. Dardari, A. Conti, J. Lien, and M. Z. Win, "The effect of cooperation on localization systems using UWB experimental data," *EURASIP J. Appl. Signal Process.*, vol. 2008, no. 1, pp. 513 873-1–513 873-11, Feb. 2008.
[34] B. Alavi and K. Pahlavan, "Modeling of the TOA-based distance measurement error using UWB indoor radio measurements," *IEEE Commun. Lett.*, vol. 10, no. 4, pp. 275–277, Apr. 2006.
[35] S. Maranò, W. M. Gifford, H. Wymeersch, and M. Z. Win, "NLOS identification and mitigation for localization based on UWB experimental data," *IEEE J. Sel. Areas Commun.*, vol. 28, no. 7, pp. 1026–1035, Sep. 2010.
[36] A. Conti, M. Guerra, D. Dardari, N. Decarli, and M. Z. Win, "Network experimentation for cooperative localization," *IEEE J. Sel. Areas Commun.*, vol. 30, no. 2, pp. 467–475, Feb. 2012.
[37] Z. Xiong, F. Sottile, M. Spirito, and R. Garello, "Hybrid indoor positioning approaches based on WSN and RFID," in *Proc. 4th IFIP Int. Conf. NTMS*, Feb. 2011, pp. 1–5.
[38] J. Youssef, B. Denis, C. Godin, and S. Lesecq, "Loosely-coupled IR-UWB handset and ankle-mounted inertial unit for indoor navigation," in *Proc. IEEE Int. Conf. Ultra-Wideband*, Bologna, Italy, Sep. 2011, pp. 160–164.
[39] D. Dardari and F. Sottile, "WPR.B database: Annex of N++ deliverable WPR.B DB.3. Progress Report II on Advanced Localization and Positioning Techniques: Data Fusion and Applications," Deliverable Number: DB.3 Annex, 216715 Newcom++, WPR.B.
[40] M. S. Arulampalam, S. Maskell, N. Gordon, and T. Clapp, "A tutorial on particle filters for online nonlinear/non-Gaussian Bayesian tracking," *IEEE Trans. Signal Process.*, vol. 50, no. 2, pp. 174–188, Feb. 2002.
[41] A. Conti, M. Z. Win, M. Chiani, and J. H. Winters, "Bit error outage for diversity reception in shadowing environment," *IEEE Commun. Lett.*, vol. 7, no. 1, pp. 15–17, Jan. 2003.

Andrea Conti (S'99–M'01–SM'11) received the Laurea degree in telecommunications engineering (*summa cum laude*) and the Ph.D. degree in electronic engineering and computer science from the University of Bologna, Bologna, Italy, in 1997 and 2001, respectively.

In 2005, he joined the University of Ferrara, Ferrara, Italy, where he is a Professore Aggregato. He was a Researcher with the Consorzio Nazionale Interuniversitario per le Telecomunicazioni in 1999–2002 and with the Istituto di Elettronica e di Ingegneria dell'Informazione e delle Telecomunicazioni, Consiglio Nazionale delle Ricerche, in 2002–2005 with the Research Unit of Bologna. In summer 2001, he was with the Wireless Systems Research Department, AT&T Research Laboratories. Since 2003, he has been a frequent visitor at the Wireless Communication and Network Sciences Laboratory, Massachusetts Institute of Technology, Cambridge, MA, USA, where he presently holds the Research Affiliate appointment. He is the coauthor of *Wireless Sensor and Actuator Networks: Enabling Technologies, Information Processing and Protocol Design* (Elsevier, 2008). His research interests involve theory and experimentation of wireless systems and networks including network localization, adaptive diversity communications, cooperative relaying techniques, interference characterization, and sensor networks.

Dr. Conti is currently an Editor of the IEEE COMMUNICATIONS LETTERS and the IEEE WIRELESS COMMUNICATIONS LETTERS. He served as an Editor of the IEEE TRANSACTIONS ON WIRELESS COMMUNICATIONS in 2003–2009 and a Guest Editor of the *EURASIP Journal on Advances in Signal Processing* (Special Issue on Wireless Cooperative Networks) in 2008. He organized and chaired a number of IEEE conferences. He is the elected Chair of the IEEE Communications Society's Radio Communications Technical Committee for 2013–2014, where he was the Vice-chair in 2011–2012 and Secretary in 2009–2010. He is an elected fellow of the IET. He has been selected as an IEEE Distinguished Lecturer. He is a recipient of the Hírközlési És Informatikai Tudományos Egyesül's Puskás Tivadar Medal and is corecipient of the IEEE Communications Society's Fred W. Ellersick Prize and of the IEEE Communications Society's Stephen O. Rice Prize in the Field of Communications Theory.

Davide Dardari (M'95–SM'07) received the Laurea degree in electronic engineering (*summa cum laude*) and the Ph.D. degree in electronic engineering and computer science from the University of Bologna, Bologna, Italy, in 1993 and 1998, respectively.

He is an Associate Professor with the University of Bologna, Cesena, Italy, where he participates in the Wireless Communications Laboratory. Since 2005, he has been a Research Affiliate with the Massachusetts Institute of Technology, Cambridge, USA. He is also a Research Affiliate with the National Research Council (IEIIT/CNR) and Consorzio Nazionale Interuniversitario per le Telecomunicazioni (CNIT). He published more than 100 technical papers and played several important roles in various national and European projects. He is coauthor of the books *Wireless Sensor and Actuator Networks: Enabling Technologies, Information Processing and Protocol Design* (Elsevier, 2008) and *Satellite and Terrestrial Radio Positioning Techniques—A Signal Processing Perspective* (Elsevier 2011). Recently, he has focused his activity on ultrawide bandwidth (UWB) systems, ranging and localization techniques, and wireless sensor networks.

Prof. Dardari is the current Chair of the Radio Communications Committee of the IEEE Communication Society. He was Cogeneral Chair of the 2011 IEEE International Conference on Ultra-Wideband. He was also the Cochair of the Wireless Communications Symposium of the 2007 IEEE International Conference on Communications, and the Cochair of the 2006 IEEE International Conference on Ultra-Wideband. He served as the Lead Editor of the *EURASIP Journal on Advances in Signal Processing* (Special Issue on Cooperative Localization in Wireless Ad Hoc and Sensor Networks) and a Guest Editor of PROCEEDINGS OF THE IEEE (Special Issue on UWB Technology & Emerging Applications) and *ELSEVIER Physical Communication Journal* (Special Issue on Advances in UWB Wireless Communications). He served as an Editor of the IEEE TRANSACTIONS ON WIRELESS COMMUNICATIONS from 2006 to 2012. He received the IEEE Communications Society Fred W. Ellersick Prize in 2012 and the IEEE Aerospace and Electronic Systems Societys M. Barry Carlton Award in 2011.

Matteo Guerra received the Laurea degree in electronics and telecommunications engineering (*summa cum laude*) from the University of Ferrara, Ferrara, Italy, in 2011, where he is currently working toward the Ph.D. degree.

Since 2010, he has been a Research Collaborator with the Telecommunications Group, University of Ferrara, working on localization techniques within the framework of the project WEBS. His research interests include theory and experimentation of location-aware wireless networks.

Mr. Guerra served as a member of the local organization committee for the 2011 IEEE International Conference on Ultra-Wideband and as a reviewer for numerous IEEE journals and international conferences.

Lorenzo Mucchi (M'98–SM'12) received the Dr.Eng. degree (Laurea) in telecommunications engineering from the University of Florence, Florence, Italy, in 1998 and the Ph.D. degree in Telecommunications and Information Society in 2001.

Since 2001, he has been a Research Scientist with the Department of Electronics and Telecommunications, University of Florence, where he has been a Professor of information technologies since 2008. During the academic year 2000–2001, he spent a 12-months period of research at the Centre for Wireless Communications, University of Oulu, Oulu, Finland. His main research areas are spread spectrum techniques (ultrawide bandwidth and code-division multiple access), cooperative communication systems, cognitive radio, wireless security, multi-input-multi-output and diversity techniques, and multisatellite communications. He has currently published 6 chapters in 6 different international books, 18 papers in international journals, and several papers in international conference proceedings during his research activity.

Dr. Mucchi is a permanent member of the Technical Committee on Telecommunications of the International Association of Science and Technology for Development. Since 2004, he has been in the technical program committee for several international conferences.

Moe Z. Win (S'85–M'87–SM'97–F'04) received the B.S. degree in electrical engineering (*magna cum laude*) from Texas A&M University, College Station, TX, USA, in 1987, the M.S. degree in electrical engineering from the University of Southern California (USC), Los Angeles, CA, USA, in 1989, and the M.S. degree in applied mathematics and the Ph.D. degree in electrical engineering as a Presidential Fellow from the USC in 1998.

He is a Professor with the Massachusetts Institute of Technology (MIT), Cambridge, MA, USA. Prior to joining MIT, he was at the AT&T Research Laboratories for five years and at the Jet Propulsion Laboratory for seven years. His research encompasses fundamental theories, algorithm design, and experimentation for a broad range of real-world problems. His current research topics include network localization and navigation, network interference exploitation, intrinsic wireless secrecy, adaptive diversity techniques, and ultrawide bandwidth systems.

Dr. Win is an elected Fellow of the AAAS and the IET. He was an IEEE Distinguished Lecturer. He is an elected Member-at-Large of the IEEE Communications Society Board of Governors in 2011–2013. He was the Chair and the Secretary of the Radio Communications Committee of the IEEE Communications Society in 2004–2006 and 2002–2004, respectively. Over the last decade, he has organized and chaired numerous international conferences. He is currently an Editor-at-Large of the IEEE WIRELESS COMMUNICATIONS LETTERS and serves on the Editorial Advisory Board of the IEEE TRANSACTIONS ON WIRELESS COMMUNICATIONS. He served as an Editor of the IEEE TRANSACTIONS ON WIRELESS COMMUNICATIONS in 2006–2012, and served as an Area Editor and an Editor of the IEEE TRANSACTIONS ON COMMUNICATIONS in 2003–2006 and 1998–2006, respectively. He was a Guest Editor of the PROCEEDINGS OF THE IEEE in 2009 and IEEE JOURNAL ON SELECTED AREAS IN COMMUNICATIONS in 2002. He was honored with two IEEE Technical Field Awards: the IEEE Kiyo Tomiyasu Award in 2011 and the IEEE Eric E. Sumner Award in 2006 (jointly with R. A. Scholtz). Together with students and colleagues, his papers have received numerous awards including the IEEE Communications Society's Stephen O. Rice Prize in 2012, the IEEE Aerospace and Electronic Systems Society's M. Barry Carlton Award in 2011, the IEEE Communications Society's Guglielmo Marconi Prize Paper Award in 2008, and the IEEE Antennas and Propagation Society's Sergei A. Schelkunoff Transactions Prize Paper Award in 2003. The highlights of his international scholarly initiatives are the Copernicus Fellowship in 2011, the Royal Academy of Engineering Distinguished Visiting Fellowship in 2009, and the Fulbright Fellowship in 2004. Other recognitions include the *Laurea Honoris Causa* from the University of Ferrara in 2008, the Technical Recognition Award of the IEEE ComSoc Radio Communications Committee in 2008, and the U.S. Presidential Early Career Award for Scientists and Engineers in 2004.